Nonlinear spectral imaging microscopy of rabbit aortic wall

Quangang Liu (刘全纲), Jianxin Chen (陈建新)*, Shuangmu Zhuo (卓双木), Xingshan Jiang (姜兴山), and Kecheng Lu (卢可成)

Institute of Laser and Optoelectronics Technology, Fujian Provincial Key Laboratory for Photonics Technology, Key Laboratory of Optoelectronic Science and Technology for Medicine of Ministry of Education, Fujian Normal University, Fuzhou 350007

**E-mail: chenjianxin@fjnu.edu.cn*

Received September 8, 2008

Employing nonlinear spectral imaging technique based on two-photon-excited fluorescence and second-harmonic generation (SHG) of biological tissue, we combine the image-guided spectral analysis method and multi-channel subsequent detection imaging to map and visualize the intrinsic species in a native rabbit aortic wall. A series of recorded nonlinear spectral images excited by a broad range of laser wavelengths (730 − 910 nm) are used to identify five components in the native rabbit aortic wall, including nicotinamide adenine dinucleotide (NADH), elastic fiber, flavin, porphyrin derivatives, and collagen. Integrating multi-channel subsequent detection imaging technique, the high-resolution, high contrast images of collagen and elastic fiber in the aortic wall are obtained. Our results demonstrate that this method can yield complementary biochemical and morphological information about aortic tissues, which have the potential to determine the tissue pathology associated with mechanical properties of aortic wall and to evaluate the pharmacodynamical studies of vessels.

OCIS codes: 170.6510, 170.4580, 300.6410.

doi: 10.3788/COL20090703.0240.

One remarkable success of multi-photon microscopy (MPM) is to open the possibility to image native biological tissues based on autofluorescence and harmonic generation of tissue intrinsic species[1]. Many intrinsic species in biological specimens such as elastic fiber, collagen, tryptophan, nicotinamide adenine dinucleotide (NADH), flavin, porphyrins, and porphyrin derivatives can fluoresce when irradiated by light of certain wavelength[1−3]. Collagen, muscle, myosin, and microtubules with noncentrosymmetric molecular organizations make them easily produce the optical second-harmonic generation (SHG)[4]. At present, two-photon excited fluorescence (TPEF) and SHG are usually the primary signal sources for forming images in MPM. Although TPEF and SHG are two completely different nonlinear light-matter interaction processes, they can simultaneously occur when the ultrashort laser pulses irradiate the biological tissue. Thus, the two nonlinear optical responses can be detected simultaneously and provide complementary information for structural and physiological investigations of tissues[1−7]. The combined TPEF/SHG research in the backward direction is the basis for clinical pathology. Moreover, the emission spectroscopy of intrinsic species is also a useful method to map intrinsic species and detect the changes of their emission intensity associated with various physiological processes such as cancer development, aging, and photoaging[8−10]. A limited number of groups have applied nonlinear microscopic imaging and spectroscopy to investigate the microstructure of tissue samples. Recently, spectroscopic measurement can be combined with MPM, which can simultaneously acquire the image of tissue specimens and the corresponding spectrum[11−13]. This is so-called spectral resolved imaging. It has been proved to be a very powerful approach for tissue biochemical analysis[11−13].

In this letter, the distribution and contents of the main species of extracellular matrix and cellular structure in a native rabbit aortic wall are investigated by using the nonlinear spectral imaging technique with the image-guided spectral analysis method. Combined with multi-channel subsequent detection imaging technique, the high resolution, high contrast images of collagen and elastic fibers in the rabbit aortic wall are acquired.

Rabbit aortas were examined in this experiment. The specimen of rabbit aorta was excised from live experimental rabbits provided from Affiliated Xiehe Hospital of Fujian Medical University. Three types of specimens were prepared, which were sandwiched between the cover glass and microscope slide. The first and second types of samples were used to image the adventitia and media when the aorta was opened longitudinally and laid between the cover glass and microscope slide with the luminal side rearing and facing the objective, respectively. The third type of sample was used to image the range from the adventitia to media along the direction perpendicular to the lumen of the aorta. The relative locations of biological samples and laser irradiation direction are shown in Fig. 1. The downward arrows represent the direction of laser irradiation. To avoid dehydration or shrinkage

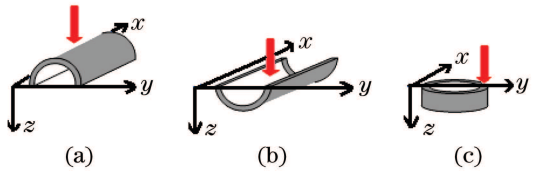

Fig. 1. Relative locations of biological samples and laser irradiation direction. The downward arrows represent the direction of laser irradiation.

during the whole imaging process, the specimens were sprinkled with phosphate buffered saline (PBS) solution (pH7.4).

The spectral imaging system used in this study has been described in detail previously[2], which is a Zeiss LSM 510 META system mounted on an Axiovert 200M inverted laser scanning microscope and coupled to a Coherent Ti:sapphire laser (110-fs pulse width, 700−980 nm tunable wavelength range). In this system, the META detector replaces the optical band pass filters and photomultiplier tube (PMT) that comprise the first channel in the standard LSM 510 scan module[3]. The META detector consists of a high-quality, reflective grating and an optimized 32-channel PMT array detector. In the Lambda mode, the emission signals from biological samples are directed onto a wavelength-dispersive element and imaged on a 32-channel detector. That means x-y images at a series of emission wavelengths are obtained. It is so-called spectral imaging. The spectral imaging technique in this system is different from that in recent reports, which consists of two dispersion prisms and a charge-coupled device (CCD) camera[13]. Based on the obtained spectral images, we acquired emission spectra of various regions of interest (ROIs) by plotting the mean intensity of all pixels with the image versus the center wavelength of each emission band, which is the image-guided spectral analysis method. In the multi-channel mode, there are eight channels behind the META detector. The spectral range of each channel can be randomly selected between $377-716$ nm by using the META detector slider. The parameter settings of each channel such as the laser intensity, the detection gain, the amplifier offset, and the amplifier gain, are relatively independent. This is the key to obtain high contrast, high resolution TPEF/SHG images. It is the multi-channel subsequent detection imaging technique. Compared with the previous combined TPEF/SHG imaging, this technique used the META detector (the dispersed light technique of grating) instead of conventional pass filters to collect emission signals from biological samples[5,6,14,15]. A Plan-Apochromat 63× (numerical aperture NA = 1.4) oil immersion objective (Zeiss) was employed for collecting the backward signals. In this letter, all images were 512×512 pixels and had a 12-bit pixel depth. The images were acquired at 2.56 μs per pixel. The average laser power at the specimen was maintained < 10 mW and no photobleaching was observed at this low power level.

To map the origin of intrinsic signal from the native aortic wall, the Ti:sapphire laser was tuned to various excitation wavelengths, λ_{ex}, throughout its tuning range (namely, 730−910 nm with increments of 10 nm), and the nonlinear spectral images were acquired. The relative location of biological samples and laser irradiation direction are shown in the Fig. 1(c). Figure 2 shows the representative nonlinear spectral images covering the region from the adventitia to near intima of the native aortic wall for $\lambda_{ex} = 730$, 810, 870 nm. And the corresponding spectra of two ROIs reflect the emission signals of the adventitia and media of native aortic wall. The spectra have been corrected for the wavelength-dependent instrument response and dark noise spectra were subtracted from the acquired sample spectrum. The emission spectrum was normalized to the maximal peak intensity.

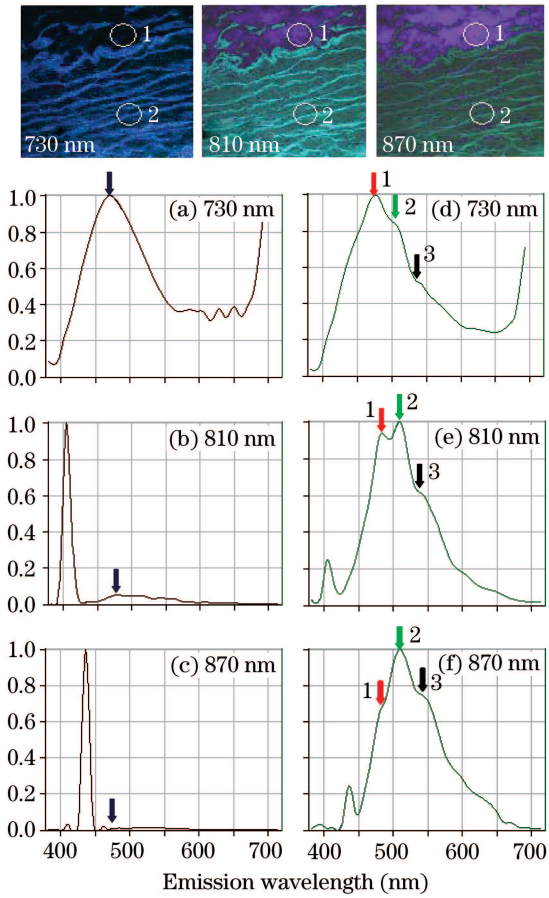

Fig. 2. Representative real-color RGB representations of the nonlinear spectral images covering the region from the adventitia to near intima of the native aortic wall for 730-, 810-, and 870-nm laser excitations. The corresponding spectra of two ROIs reflect the emission signals of the adventitia and media of the native aortic wall. All spectra are normalized to their maximal peak intensities. (a)—(c) for the ROI 1; (d)—(f) for the ROI 2.

In the ROI 1 (in the adventitia), for $\lambda_{ex} = 870$ nm, the spectrum exhibits a sharp peak with a narrow width, as shown in Fig. 2(c). Through the Gaussian curve fitting analysis, the peak is located at 435 nm, which is at precisely half the excitation wavelength. This is characteristic of the nonlinear optical effect of SHG. According to the previous study of collagen and the aorta histology[14,16], we conclude that collagen in the adventitia of aortic wall is responsible for the SHG signal. In real-color RGB representations of the spectral images, it can be seen that the purple color reflects the backscattered-second-harmonic signal generated by collagen (colorful images are not given here). For $\lambda_{ex} = 810$ nm, the corresponding emission spectrum in the ROI 1 presents not only a sharp 405-nm SHG peak but also a broad band in the $425-650$ nm region with very weak intensity, which originates from the TPEP of collagen. For $\lambda_{ex} = 730$ nm, we could not acquire the whole SHG signal due to our system's limitation, but the part of SHG signal at near 377 nm could be seen. Moreover, the strong TPEF signal originating from collagen with a 475-nm peak in the $400-716$ nm region was observed. These results show that at longer excitation wavelengths (> 800 nm), the signal emitted from collagen is exclu-

sively due to SHG, whereas at the shorter excitation wavelengths the collagen signal is a combination of SHG and TPEF signals.

In the ROI 2 (in the media), for $\lambda_{ex} = 870$ nm, the whole spectrum can be divided into two distinct ranges according to the spectral shape. The first range has only one peak with a narrow width. From the above discussion, it is known that the sharp peak signal at 435 nm originates from the SHG of collagen. From the real-color RGB representations of the spectral image in the media, it can also be seen that the purple color arises from the backscattered-second-harmonic signal generated by collagen. The other range shows a broad feature from 450 to 716 nm with three peaks at 475, 510, 535 nm. It was demonstrated in previous works[2,3,8] that cellular NADH, elastic fiber, and cellular flavin contribute to the three peaks. Specifically, NADH fluorescence is responsible for the 475-nm peak (arrow 1 marked). The 510-nm peak (arrow 2 marked) corresponds to the elastic fiber fluorescence and elastic fibers in the aorta exhibit the morphology of lamella. And the 535-nm peak (arrow 3 marked) is associated with the presence of cellular flavin. As can be seen from Figs. 2(d)—(f), for $\lambda_{ex} = 870$ nm, the relative TPEF intensities of cellular NADH is lower than that of elastic fiber; for $\lambda_{ex} = 810$ nm, the relative TPEF intensity of cellular NADH is nearly equal to that of elastic fiber; but for $\lambda_{ex} = 730$ nm, the relative TPEF intensity of cellular NADH exceeds that of elastic fiber. At the same time, for different excitation wavelengths, the real-color RGB representations of the media have changed correspondingly.

Additionally, it was found that there was a special peak at 700 nm for $\lambda_{ex} = 770$ nm. This peak does not exist at other wavelength laser excitations (the data are not shown). It was reported in previous studies[8,11] that the 700-nm peak may be responsible for porphyrin derivatives. Using the nonlinear spectral imaging technique integrated with an image-guided spectral analysis method, we identify five factors that contribute to most of the intrinsic signals from the aortic wall, including NADH, elastic fiber, flavin, porphyrin derivatives, and collagen. These results show that it is a very useful technique to map intrinsic species of biological tissues.

According to the above discussion, it is known that collagen and elastic fiber are the main structural components of the adventitia and media in the aortic wall. Their structural modifications are tightly associated with mechanical properties of aorta wall and pharmacodynamical studies of vessels[16]. But there is a lack of high contrast three-dimensional rendering of the structure of collagen and elastic fiber. Here we present high contrast images of the structure of collagen and elastic fiber by using the multi-channel subsequent detection imaging technique. It is clear that the efficiencies of TPEF from collagen, porphyrin derivatives, cellular NADH, and flavin are much lower than that of elastic fibers when 870-nm excitation light is used. But collagen is responsible for the strong SHG signal that has a sharp 435-nm peak with 11.7-nm width. That means the SHG signals from collagen can be spectrally isolated from TPEF from elastic fibers. TPEF from elastic fibers can be used to image elastic fibers, avoiding the interference of TPEF from collagen, porphyrin derivatives, cellular NADH, and flavin. Using two channels behind the META detector, the combined images of collagen and elastic fiber with excellent contrast and specificity can be obtained. Using the META detector slider, the detection spectral ranges were set in a narrow band (430 − 440 nm) for imaging SHG of collagen and a broad band (450 − 650 nm) for imaging TPEF of elastic fibers, respectively. The laser excitation power, detection gain, amplifier offset, and amplifier gain of two channels were set with different parameters during the imaging process in order to ensure the optimal imaging condition of collagen and elastic fiber detected in different channels. This can further enhance their imaging contrast. This is an advantage of the multi-channel subsequent detection imaging technique.

Figures 3(a)—(d) present the high contrast, high resolution images of collagen and elastic fiber in the adventitia, the media near adventitia, the media near intima, and the range from adventitia to media, respectively. The relative locations of biological samples and laser irradiation direction are presented in Figs. 1(a), 1(b), and 1(c), respectively. With colorful images, red image arising from the SHG signal of collagen can be clearly distinguished from the green image originating from the TPEF signal of elastic fiber. Especially, a little elastic fiber in the adventitia and a little collagen in the media can be clearly seen. From Figs. 3(b) and (c), it is found that the elastic fiber density in the media near intima is greater than that in the media near adventitia.

In this letter, we demonstrate that the combination of nonlinear spectral imaging technique with an image-guided spectral analysis method and a multi-channel subsequent detection imaging technique can yield complementary biochemical and morphological information about aortic tissues that no individual technique can provide by itself. The combined technique reported here opens many possibilities to enhance our understanding of vascular biomechanics in health and various disease processes such as hypertension, diabetes, and atherosclerosis. The technique also has the potential to evaluate pharmacodynamical studies of vessels. This technique

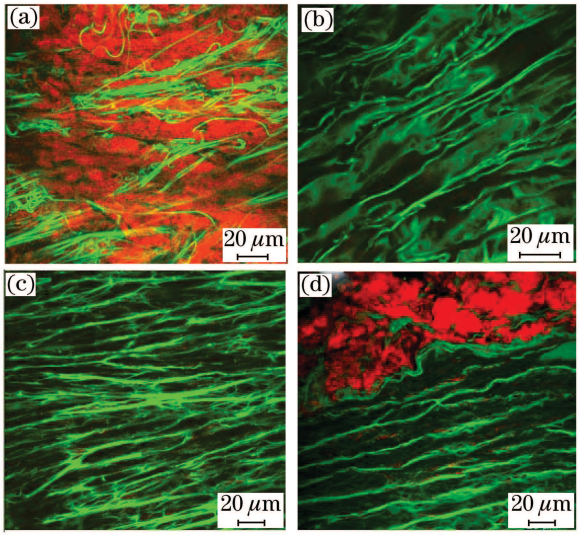

Fig. 3. High contrast images of collagen and elastic fiber. (a) In the adventitia; (b) in the media near the adventitia; (c) in the media near intima; (d) in the range from adventitia to media.

has also been extended to investigate the physiology and pathology of epithelial tissue, proving that autofluorescence spectra and morphometric alterations of the epithelial layer are strongly correlated to epithelial carcinogenesis[3,5,11].

This work was supported by the National Natural Science Foundation of China (No. 60508017), the Natural Science Foundation of Fujian Province (No. 2007J0007, C0720001), the Science and Technology Planning Key Program of Fujian Province (No. 2008Y0037), and the Program for New Century Excellent Talents in University of China (NCET-07-0191).

References

1. G. Boyer and K. Plamann, Chin. Opt. Lett. **5,** 477 (2007).
2. S. Zhuo, J. Chen, T. Luo, D. Zou, and J. Zhao, Opt. Express **14,** 7810 (2006).
3. S. Zhuo, J. Chen, B. Yu, X. Jiang, T. Luo, Q. Liu, R. Chen, and S. Xie, J. Biomed. Opt. **13,** 054024 (2008).
4. P. J. Campagnola and L. M. Loew, Nature Biotechnol. **21,** 1356 (2003).
5. S. Zhuo, J. Chen, X. Jiang, S. Xie, R. Chen, N. Cao, Q. Zou, and S. Xiong, Phys. Med. Biol. **52,** 4967 (2007).
6. S. Zhuo, J. Chen, N. Cao, X. Jiang, S. Xie, and S. Xiong, Phys. Med. Biol. **53,** 3317 (2008).
7. S. Zhuo, J. Chen, X. Jiang, K. Lu, and S. Xie, Laser Phys. Lett. **5,** 614 (2008).
8. R. Richards-Kortum and E. Sevick-Muraca, Annu. Rev. Phys. Chem. **47,** 555 (1996).
9. J. Chen, S. Zhuo, T. Luo, and J. Zhao, Chin. Opt. Lett. **4,** 598 (2006).
10. J. Chen, S. Zhuo, T. Luo, X. Jiang, and J. Zhao, Scanning **28,** 319 (2006).
11. J. Chen, S. Zhuo, R. Chen, X. Jiang, S. Xie, and Q. Zou, New J. Phys. **9,** 212 (2007).
12. S. Zhuo, J. Chen, X. Jiang, X. Cheng, and S. Xie, Skin Res. Technol. **13,** 406 (2007).
13. J. A. Palero, H. S. de Bruijn, A. van der Ploeg-van den Heuvel, H. J. C. M. Sterenborg, and H. C. Gerritsen, Opt. Express **14,** 4395 (2006).
14. J. Chen, S. Zhuo, T. Luo, D. Liu, and J. Zhao, Optik **119,** 519 (2008).
15. S. Zhuo, J. Chen, X. Jiang, T. Luo, R. Chen, S. Xie, and Q. Zou, Scanning **29,** 219 (2007).
16. T. Boulesteix, A.-M. Pena, N. Pagès, G. Godeau, M.-P. Sauviat, E. Beaurepaire, and M.-C. Schanne-Klein, Cytometry A **69,** 20 (2005).